

Observations implicating vibronic coupling in covalently linked transition metal electron transfer systems

John F. Endicott *, Murielle A. Watzky, Xiaoqing Song, Tione Buranda

Department of Chemistry, Wayne State University, Detroit, MI 48202-3489, USA

Received 22 December 1995

Contents

1. Introduction	296
2. Semi-classical approaches to (D–A)-electron transfer systems	297
3. Some transient studies of BET in D–A systems	300
4. Systematic studies of D–A couplings in strongly coupled complexes	300
4.1. Background and a simple basis for experimental comparisons	303
4.1.1. Concerning the definition of $E_{1/2}^{ref}$	303
4.1.2. Contributions to e_2^{th}	305
4.2. Systematic comparisons of D–A coupling inferred from spectroscopic and electrochemical measurements	306
4.2.1. Studies based on perturbational changes in non-bridging ligands	306
4.2.2. Studies based on the variations of the coupled metals with the ligands held constant	306
4.2.3. The role of symmetry in the comparison of e_2^{th} and e_2^{op}	307
4.2.4. Red shift of the cyanide stretching frequencies in CN-bridged D–A complexes	311
4.2.5. Charge-transfer spectroscopy of the CN-bridged complexes: coupling and mixing of chromophores	311
4.2.6. Variations in the solvational contributions to $E_{1/2}^{obsd}$	314
4.2.7. Spin multiplicity contributions and other effects of M–M' coupling	314
4.2.8. Changes in vibrational frequencies and zero-point energy differences	315
4.3. The effect of the estimated correction terms on the correlation of $E_{1/2}^{obsd}$ with e_2^{op}	315
4.4. Summary: some experimental consequences of strong D–A coupling	315
5. A simple vibronic approach to D–A coupling	316
6. Summary and conclusions	320
6.1. Some implications of vibronic coupling	320
6.2. Extensions to other systems	320
Acknowledgements	321
References	321

* Corresponding author.

Abstract

Experimental observations on the properties and photophysical behavior of several bimetallic and trimetallic donor–acceptor (D–A) complexes are considered. Photoinduced charge separation followed by back electron transfer seems to conform well to the behavior inferred from Born–Oppenheimer-based perturbation theory models when D–A coupling is weak, $\beta_{DA} < 100 \text{ cm}^{-1}$, but not when D–A coupling is very strong, $\beta_{DA} > 10^3 \text{ cm}^{-1}$. The best documented examples of deviations from the expected behavior are drawn from CN^- -bridged transition metal systems, and this same class of D–A complexes also exhibits anomalous ground state properties: (a) a shift to lower energy, which is a function of D–A coupling, of the bridging CN^- stretching frequency only when a donor and an acceptor are bridged; (b) a much larger than expected, (based on D–A charge transfer absorption) thermodynamic stabilization. Related behavior of strongly coupled D–A complexes with larger bridging ligands has also been reported. It is pointed out that substitution of a vibronic perturbation for the purely electronic perturbation of Born–Oppenheimer-based models can at least partially account for these observations. The vibronic model employed involves ligand to metal charge transfer (LMCT) and metal to ligand (MLCT) charge transfer interactions with nearest neighbor donor and acceptor respectively. The pertinent LMCT and MLCT parameters are, in principle, measurable, and their magnitudes seem compatible with the observed behavior. Some further implications and extensions are considered. © 1997 Elsevier Science S.A.

Keywords: Vibronic coupling; Born–Oppenheimer-based perturbation models; D–A complexes; LMCT; MLCT

1. Introduction

One approach to simple molecular photosystems in which the maximum amount of actinic energy might be converted to chemical energy is based on the efficient, light-induced separation of charge within a molecular donor–acceptor (D–A) complex [1–3]. Covalently linked, transition metal complexes could provide good models for such processes. However, in order for the conversion of light-to-chemical energy to be useful, one must find a means of repressing the back electron transfer (BET) reaction; Fig. 1 illustrates the issues for a ruthenium-based D–A complex. The rate constant for BET is given in the semi-classical limit by Eq. (1) [2,3]

$$k_{\text{BET}} = \kappa_{\text{el}} \kappa_{\text{nu}} \nu_{\text{eff}} \quad (1)$$

where the κ_i are transmission (or retardation) coefficients (el=electronic; v=nuclear) and ν_{eff} is the intrinsic frequency of BET in the absence of electronic or nuclear retardation. For maximum energy storage one would expect $\kappa_{\text{nu}} \approx 1$, so that any retardation of BET would have to arise from κ_{el} . In order to design systems in which $\kappa_{\text{el}} < 1$, one must first understand how molecular properties contribute to its magnitude. The clear experimental determination of these contributions has been difficult, but it is a subject of much interest [3–13].

Some recent studies of strongly coupled D–A complexes have made systematic comparisons of spectroscopic and thermodynamic determinations of the coupling

Photogeneration of Charge Separated Intermediates

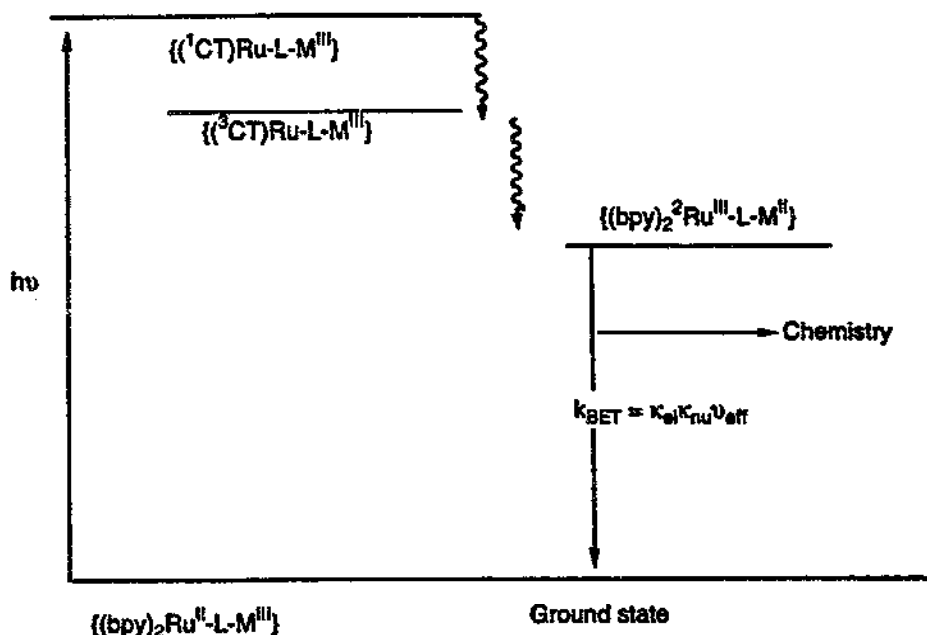


Fig. 1. Schematic diagram illustrating the principle steps in the photogeneration of charge separated intermediates. This particular example is based on the photophysics of ruthenium–polypyridyl complexes.

strength, and these comparisons have *not* been in good agreement with the Born–Oppenheimer-based logic which is exemplified in Eq. (1) [14–19]. Other studies of some complexes, discussed below, also raise the question of limits of applicability of Eq. (1) to strongly coupled D–A systems. In this article we review these experimental studies, and we point out that the discrepancies between them and semi-classical theoretical models can be at least qualitatively resolved by substituting the simple vibronic assumption that electronic and nuclear motions are linearly coupled for the Born–Oppenheimer assumption that they are separable.

2. Semi-classical approaches to (D–A)-electron transfer systems

Eq. (1) and the related semi-classical or quantum mechanical theoretical models have been very successful in accounting for most of the experimental observations on weakly-coupled, outer-sphere (bimolecular) electron transfer reactions [2, 20–22]. The systematic studies of weakly-coupled, covalently linked D–A systems have mostly involved organic donors and acceptors, and these studies have largely conformed to expectation based on Eq. (1) [6, 10, 23]; usually the detailed fits to Eq. (1) have been based on the quantization of the high frequency vibrational modes contributing to κ_{nu} , and the inefficient energy exchange between high and low

frequency modes, while the nuclear reorganizational and electronic coupling parameters ($\kappa_{el} < 1$) have usually been treated as adjustable. One advantage of using covalently linked transition metals in a D–A complex is that one can make ready comparisons to the outer-sphere electron transfer data and that nuclear reorganizational energies can often be independently evaluated through a combination of the bimolecular kinetic data and structural data. In principle, the electronic coupling may also be independently evaluated, so that one ought to be able to compare observed values of k_{BET} with the values expected based on independently determined nuclear reorganizational and electronic coupling parameters.

The theoretical basis for structure–reactivity correlations in simple outer-sphere electron transfer systems has been extensively reviewed [1–4,20–22] and only the most pertinent features will be mentioned here.

In a strictly classical, adiabatic limit, $\kappa_{el} \approx 1$, and κ_{nu} is given by Eq. (2)

$$RT \ln \kappa_{nu} = (\lambda_{DA}/4)(1 + \Delta G_{DA}^\ominus/\lambda_{DA})^2 \quad (2)$$

where λ_{DA} is a nuclear reorganizational parameter (see Fig. 2) and ΔG_{DA}^\ominus is the standard free energy difference between the ground state electronic configuration (i.e. D⁺A) and the configuration with the electron in an acceptor orbital (DA[−]) [1,2,20,22,24]. In this same limit the energy of the donor–acceptor charge transfer (DACT) absorption maximum is given by Eq. (3).

$$h\nu_{op} \approx |\Delta E_{DA}^\ominus| + \lambda_{DA} \quad (3)$$

The non-adiabatic, limit, $\kappa_{el} < 1$, may be treated semi-classically to obtain Eq. (4) [2,22]

$$\kappa_{el} = 2(H_{DA}^2/h\nu_{eff})(\pi^3/\lambda_{DA}RT)^{1/2} \quad (4)$$

where H_{DA} is the D–A coupling matrix element ($H_{DA} = \langle \Psi_{DA} | H | \Psi_A \rangle$), where the

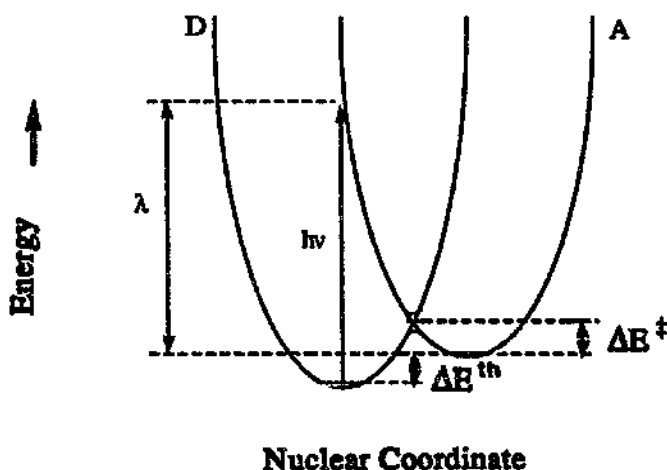


Fig. 2. Qualitative potential energy surfaces for a simple electron transfer system.

Ψ_i are the respective state wave functions and H' is the perturbational Hamiltonian which allows the mixing). In this same limit the oscillator strength of the DACT absorbance is also proportional to H_{DA}^2 [3,25–27]. For our purposes it is more consistent to express the mixing coefficient, $\beta_{DA}/E_{DA} = \alpha_{DA}$, of the zero-order (or diabatic) donor and acceptor wave functions ($\Psi_D = \Psi_D^\ominus + \alpha_{DA} \Psi_A^\ominus$) as in Eq. (5) [26]

$$\alpha_{DA} = \beta_{DA}^\ominus / E_{DA} \approx \frac{0.0205}{r_{DA}} \left(\frac{\epsilon_{\max} \Delta\nu_{1/2}}{h\nu_{op}} \right)^{1/2} \quad (5)$$

where $\beta_{DA} = H_{DA} - SE_D^\ominus$, S is an overlap integral, E_D^\ominus is the energy of the diabatic ground state, r_{DA} is the distance between the unperturbed orbital origins, and where ϵ_{\max} and $\Delta\nu_{1/2}$ are the absorptivity and full width at half-height of the DACT absorbance. If α_{DA} is sufficiently large, as would be the case when D–A coupling is very large, then Eq. (3) may have to be modified (see Fig. 3) to take account of the ground state stabilization which results from D–A mixing.

Eq. (6)

$$h\nu_{op} \approx |E_{DA}| + 2\epsilon_s^{\text{th}} \quad (6)$$

is usually sufficient to take account of this problem when the ground state

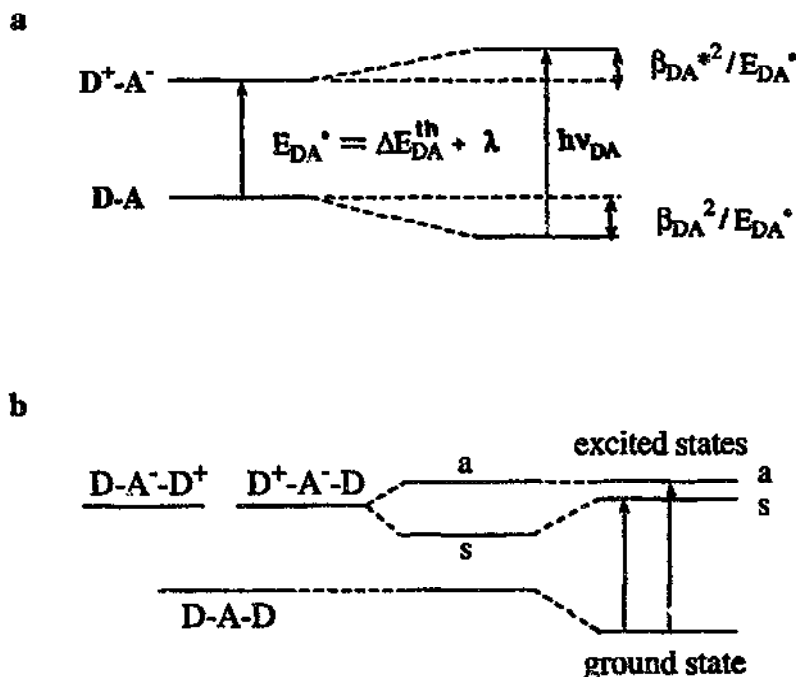


Fig. 3. Vertical energy level schemes for a simple donor–acceptor system (a), and for a degenerate donor–acceptor system (b).

stabilization energy $\varepsilon_s^{\text{th}}$ associated with D–A coupling is given by Eq. (7)

$$\varepsilon_s^{\text{th}} = (\beta_{\text{DA}}^{\text{th}})^2 / E_{\text{DA}} \quad (7)$$

and where we have distinguished the stabilization manifested in thermodynamic measurements, with a superscript th, from that which might be inferred from the DACT absorption spectrum, $\varepsilon_s^{\text{op}} \approx (\beta_{\text{DA}}^{\text{op}})^2 / E_{\text{DA}}$. In the limit discussed here, in which it is assumed that the nuclear and electronic coordinates are separable, and thus simple first order perturbational arguments are applicable, $\varepsilon_s^{\text{th}} = \varepsilon_s^{\text{op}}$. However, since these parameters are based on different kinds of measurement, their equality is subject to experimental investigation, and several such studies [14–19] have found that $\varepsilon_s^{\text{th}} > \varepsilon_s^{\text{op}}$. Such observations and their significance are the principle focus of this article.

3. Some transient studies of BET in D–A systems

Pertinent values of k_{BET} , determined by transient absorption spectroscopy for some covalently linked transition metal D–A systems, are summarized in Table 1. We have included the weakly coupled $(\text{bpy})_2\text{Ru}(\text{bb})\text{Co}(\text{bpy})_2^+$ complex in Table 1 ($\text{bb} = 1,2\text{-bis}(2,2'\text{-bipyridyl-4'-yl})\text{ethane}$; see Fig. 4) as a simple example of a weakly coupled system and for contrast with the strongly coupled CN^- -bridged complexes. The D–A coupling in this complex is estimated to be $H_{\text{DA}} \approx 80 \text{ cm}^{-1}$ based on a metal to ligand charge transfer (MLCT) mediated super exchange model [32]. This estimate, implying $\kappa_{\text{el}} \approx 10^{-2}$, together with the semi-classical logic sketched above, account very well for the magnitude of k_{BET} . This seems to be a reasonably typical example of the behavior of weakly coupled D–A systems, and it serves to illustrate the statement made above, that the semi-classical, Born–Oppenheimer-based formalisms seem to work very well for weakly coupled D–A systems.

These same semi-classical formalisms do not account for either the variations or the magnitudes of k_{BET} for the strongly coupled CN^- -bridged complexes in Table 1. Further to this point, the value of k_{BET} reported for $(\text{NC})_5\text{RuCNRu}(\text{NH}_3)_5$ [30,31] is much larger than the rate constants for vibrational relaxation in the photogenerated electron transfer excited state [30,31,33,34]. If the electronically excited system does not reach vibrational equilibrium within the excited state electronic manifold before electron transfer, then some of the assumptions of the semi-classical approach are invalid. At the very least, the observations on k_{BET} in CN^- -bridged D–A complexes raise questions about the validity of many of the interpretations of strongly coupled D–A complex properties in terms of the semi-classical formalisms sketched above.

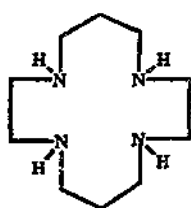
4. Systematic studies of D–A coupling in strongly coupled complexes

An experimental approach to examining the validity of relationships inferred from semi-classical arguments is to examine the consistency of perturbational parameters, e.g. β_{DA} , inferred from different physical measurements. As noted above, the semi-

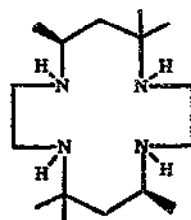
Table 1
BET behavior of some bridged donor-acceptor complexes

Complex	Ref.	BET processes ^a	$k_{\text{BET}}(\text{obsd})$ ($\text{s}^{-1}/10^{10}$)	λ_{DA} ($\text{cm}^{-1}/10^3$)	$-\Delta G_{\text{DA}}^{\text{b}}$ ($\text{cm}^{-1}/10^3$)	ΔG^{b} ($\text{cm}^{-1}/10^3$)	$\beta_{\text{DA}}^{\text{c}}$ ($\text{cm}^{-1}/10^3$)
(bpy) ₂ Ru(CNCo(NH ₃) ₃) ₂ ⁶⁺	[28]	$5.3^2[\text{Ru}^{\text{III}}\text{Co}^{\text{III}}] \rightarrow 1^2[\text{Ru}^{\text{II}}\text{Co}^{\text{III}}]$	0.3	~15	~12	0.2 ± 0.2	— ^d
(bpy) ₂ Ru(CN)(CNCo tetraen) ₂ ³⁺	[28]	$5.3^2[\text{Ru}^{\text{III}}\text{Co}^{\text{III}}] \rightarrow 1^2[\text{Ru}^{\text{II}}\text{Co}^{\text{III}}]$	0.4	~14	11.8	0.1	— ^d
(bpy) ₂ Ru(CNRu(NH ₃) ₃) ₂ ⁵⁺	[28]	$3.1^2[\text{Ru}^{\text{III}}\text{Ru}^{\text{III}}] \rightarrow 3.1^2[\text{Ru}^{\text{II}}\text{Ru}^{\text{III}}]$	> 20	3.6	11.3	4.1(2.3)	1.8
trans-Co([14]aneN ₄)(CNRu(NH ₃) ₃) ₂ ⁵⁺	[17]	$3.1^2[\text{Ru}^{\text{III}}\text{Co}^{\text{III}}] \rightarrow 1^2[\text{Ru}^{\text{II}}\text{Co}^{\text{III}}]$	0.2(0.7) ^f	7.8	12.1	0.6	1.1
trans-Cr([14]aneN ₄)(CNRu(NH ₃) ₃) ₂ ⁵⁺	[29]	$6.4^2[\text{Ru}^{\text{III}}\text{Cr}^{\text{III}}] \rightarrow 4^2[\text{Ru}^{\text{II}}\text{Cr}^{\text{III}}]$	~0.01	~8	~14	~1	1.9
(NC) ₃ Ru(CNRu(NH ₃) ₃) ₂ ⁺	[30,31]	$2^2[\text{Ru}^{\text{III}}\text{Ru}^{\text{III}}] \rightarrow 2^2[\text{Ru}^{\text{II}}\text{Ru}^{\text{III}}]$	1.2×10^3	6	8	0.2	1.4
(bpy) ₂ Ru(bb)Cr(bpy) ₂ ³⁺	[32]	$5.3^2[\text{Ru}^{\text{III}}\text{Co}^{\text{III}}] \rightarrow 1^2[\text{Ru}^{\text{II}}\text{Co}^{\text{III}}]$	0.02	13.8	7.7	2.2	~0.01 ^f

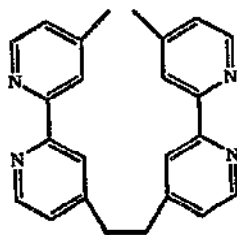
^a Possible spin multiplicities are indicated by left superscript and are based on the most probable ground state of the isolated compounds.
^b $\Delta G^{\text{b}} = (\lambda_{\text{DA}}/4)(1 + \Delta G_{\text{DA}}^{\text{b}}/\lambda_{\text{DA}})^2$; number in parentheses is $\Delta G^{\text{b}} \rightarrow \beta_{\text{DA}}^{\text{c}}$. ^c Calculated iteratively using Eqs. (5) and (6) and the assumption that $\epsilon_{\text{DA}}^{\text{b}} \approx 4\epsilon_{\text{DA}}^{\text{ex}}$; per Ru. ^d No DACT absorption observed [28]. ^e For macrocyclic ligands, see Fig. 4. ^f Calculated for $^4\text{Co}^{\text{III}}\text{--}^2\text{Ru}^{\text{III}}$ coupling from a superexchange model [32].



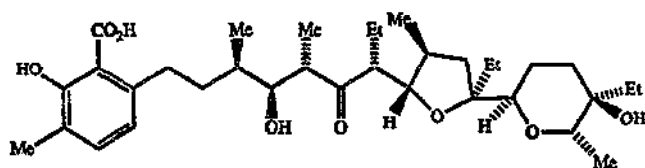
[14]aneN₄
(cyclam)



rac-(5,12) Me₆[14]aneN₄
(tet-b)



bb



lasalocid

Fig. 4. Some ligands cited in the text: [14]aneN₄=1,4,8,11-tetraazacyclotetradecane; rac-Me₆[14]aneN₄=5,12-rac-5,7,7,12,14,14-hexamethyl-1,4,8,11-tetraazacyclodecane; bb=1,2-bis(2,2'-bipyridyl-4'-yl)-ethane.

classical argument implies that β_{DA} is related in simple ways to (a) k_{BET} , (b) the oscillator strength of a DACT absorption and (c) the stability of electron transfer ground state. The DACT absorption and the ground state stability are referenced to the ground state nuclear coordinates, while k_{BET} is referenced to the electron transfer transition state nuclear coordinates. Obviously, the fewest assumptions are involved in comparisons of the DACT absorption and the effect of D–A coupling on ground state stabilization. The trends in ground state stabilization, as well as DACT absorption spectra, should be readily measurable when D–A coupling is large. Transition metal D–A complexes are useful for this purpose since they can be

synthesized with at least one component which can be reversibly oxidized or reduced, and since accurate electrochemical measurements are relatively easy to make, and they are sensitive measures of changes in stabilization of one component of the redox couple.

4.1. Background and a simple basis for experimental comparisons

There is a vast literature on D–A complexes of the type $M(BL)M'$ in which M and M' are ammine and/or imine complexes of Ru or Os with a variety of bridging ligands (BL) [2, 11, 12, 15, 20, 35–37]. Variations in DACT spectra and in electrochemical half-wave potentials ($E_{1/2}$ for M^+-M and/or M'^+-M') have been extensively examined as a function of bridging and non-bridging ligands. A wide range of DACT absorption band energies and oscillator strengths and a considerable range of values of $E_{1/2}$ for the component couples has been reported for these $D(BL)A$ complexes. When the M^+-M and M'^+-M' couples are identical, the $D(BL)A$ complexes have been found to vary from having the odd electron equally delocalized over both metal sites (e.g. for $BL=pz$) to having the odd electron predominantly trapped at a single site (e.g. for $BL=4,4'$ -o pyridine).

In this article we wish to emphasize $D(BL)A$ complexes in which the component couples differ so that the 'odd' electron is thermodynamically trapped at the donor site (typically by 1–2 eV) in the electron transfer ground state. This property should make first-order perturbational arguments relatively reliable. If measurements of $E_{1/2}$ are for one of the component couples, e.g. for the A–A couple, then the observed half-wave potential can be written as in Eq. (8)

$$E_{1/2}^{obsd} = E_{1/2}^{ref} \pm e_s^{th} \quad (8)$$

where the 'plus' sign is used when A^- is DACT stabilized and the 'minus' sign when A is stabilized by DACT coupling. In principle, the quantities in Eq. (8) are defined very simply: (a) $E_{1/2}^{ref}$ is the half-wave potential in an equivalent complex in which $\beta_{DA}=0$; (b) e_s^{th} contains all the contributions to the potential which result from D–A coupling. In practice, neither of these quantities is very simple, and the contributions to each of them should be carefully considered.

4.1.1. Concerning the definition of $E_{1/2}^{ref}$

Two experimental approaches have been used for defining $E_{1/2}^{ref}$ in complexes of the type $LM(BL)M'L'$. The most common is a synthetic approach in which a 'non-ionizable' metal for the donor, or a metal with no effective electron affinity for the acceptor, and the resulting experimental value of $E_{1/2}$ is used for the probe couple as the measure of $E_{1/2}^{ref}$. For example, if a complex of the type $LM(BL)Ru^{III}(NH_3)_5$ exhibits a DACT absorption, so that $|e_s^{th}| > 0$ and if LM^+-LM is the probe redox couple, then the measured value of $E_{1/2}$ for the LM^+-LM couple in the $LM(BL)Rh^{III}(NH_3)_5$ complex would be a reasonable experimental estimate of $E_{1/2}^{ref}$, since charge type and all ligands remain the same. A potential complication of this approach is that factors other than D–A coupling may be altered by the substitution of metals, and, if these are large enough, ' $E_{1/2}^{ref}$ ' so determined may not be an appropriate reference value for the effects of this coupling. If the systems investigated

are well described by the simple first-order perturbation theory arguments described above, and if the compounds are accessible, then there would be few serious problems with this definition of $E_{1/2}^{\text{ref}}$. If there is any synergy in the M–M' interactions with the ligands and/or solvent, or if there are M–M' interactions other than D–A coupling, then a more careful definition of $E_{1/2}^{\text{ref}}$ is in order. As an example of a possible problem of this type, consider the $\text{Ru}(\text{bpy})_2^{3+,2+}$ couple in complexes of the type $(\text{bpy})_2\text{LRu}(\text{BL})\text{M}^{\text{III}}(\text{NH}_3)_5$. When $\text{M}=\text{Ru}(\text{III})$ there could be spin–spin coupling between $\text{Ru}(\text{III})$ centers so that the contribution of spin statistics and coupling energy to the redox couple would be different for the Ru–Ru and the 'reference' couple [38]. The difference in spin statistics alone could lead to a value for $E_{1/2}^{\text{obsd}}$ for the value of the $\text{Ru}(\text{bpy})_2^{3+,2+}$ couple in the $\text{M}=\text{Rh}(\text{III})$ complex which is as much as 36 mV [39] larger than the appropriate value of $E_{1/2}^{\text{ref}}$.

Another experimental approach would be to evaluate $E_{1/2}^{\text{ref}}$ by interpolation or by extrapolation. This approach is characteristic of much of the work discussed here. In particular, this approach is appropriate for some series of $\text{LM}(\text{CN}^-)\text{Ru}(\text{NH}_3)_5$ complexes in which $\text{Ru}(\text{NH}_3)_5^{3+,2+}$ is the redox probe couple [16–19]. In the complexes studied so far $\text{Ru}(\text{NH}_3)_5^{3+}$ is stabilized by D–A coupling when $\text{M}=\text{Ru}(\text{II})$ or $\text{Fe}(\text{II})$, and $\text{Ru}(\text{NH}_3)_5^{2+}$ is stabilized when $\text{M}=\text{Cr}(\text{III})$ or $\text{Co}(\text{III})$. In such series of complexes, the effect of a one unit charge difference, at a site somewhat remote from the probe redox couple, is a factor in the evaluation of $E_{1/2}^{\text{ref}}$, and the spin statistical issues noted above will also be a factor in evaluating the $\text{Cr}(\text{III})$ complexes.

The effect of charge density on the solvational contribution to simple redox couples has been considered by Richardson [39]. Since the charge density is much greater at the $\text{Ru}(\text{NH}_3)_5$ than at the LM site of the $\text{LM}(\text{CN}^-)\text{Ru}(\text{NH}_3)_5$ complexes, one expects the effects to be small. The comparison of several complexes [16–19] suggests that 20 mV per unit of charge is a reasonable upper limit for the purely solvational effect, so that, based on this factor only, $E_{1/2}^{\text{ref}}$ would be ca. 20 mV greater for $\text{M}=\text{Rh}(\text{III})$, $\text{Co}(\text{III})$ or $\text{Cr}(\text{III})$ than for $\text{M}=\text{Fe}(\text{II})$ or $\text{Ru}(\text{II})$.

Another charge-dependent factor which can affect $E_{1/2}^{\text{ref}}$ is the electrostatic polarization [40] of electrons within the bridging ligand. The effect of this factor is undoubtedly attenuated by the solvent and by ionic association. Model compound studies can be used to set limits. The $\text{Ru}(\text{bpy})_2^{3+,2+}$ couple has been found to have a value of $E_{1/2}^{\text{ref}}$ which is 272 mV more positive (see Fig. 5) in the $(\text{bpy})_2(\text{CN})\text{Ru}(\text{CNRh}(\text{NH}_3)_5)^{4+,3+}$ couple than in the $\text{Ru}(\text{bpy})_2(\text{CN})_2^{2+,0}$ couple [16]. This is undoubtedly the result of covalent as well as electrostatic contributions, and there is undoubtedly some contribution from CN^- –solvent interactions. Nevertheless, this observation can be used to set an extreme upper limit of 100 mV per unit charge for the effect of charge change (both on solvation and on polarization) at a remote site. That this is an upper limit is demonstrated by the 212 mV greater value of $E_{1/2}^{\text{obsd}}$ [16] for the $(\text{bpy})_2\text{Ru}(\text{CNRh}(\text{NH}_3)_5)^{7+,6+}$ couple than for $(\text{bpy})_2(\text{CN})\text{Ru}(\text{CNRh}(\text{NH}_3)_5)^{4+,3+}$. An even smaller value for the polarization correction (20 mV) is implied by the shifts in central $\text{Ru} \rightarrow \text{bpy}$ MLCT and the DACT absorption maxima in $(\text{bpy})_2\text{Ru}(\text{CNRu}(\text{NH}_3)_5)_2[\text{LAS}]_6$ in which the charge is completely neutralized by association with the lasalocid anion [41], and for which Eq. (3) and Eq. (6) were used to estimate $E_{1/2}$ [42].

Electrochemical Behavior of $(\text{bpy})_2(\text{CN})_{2-n}\text{Ru}(\text{CNM}(\text{NH}_3)_5)_n^{3n+}$

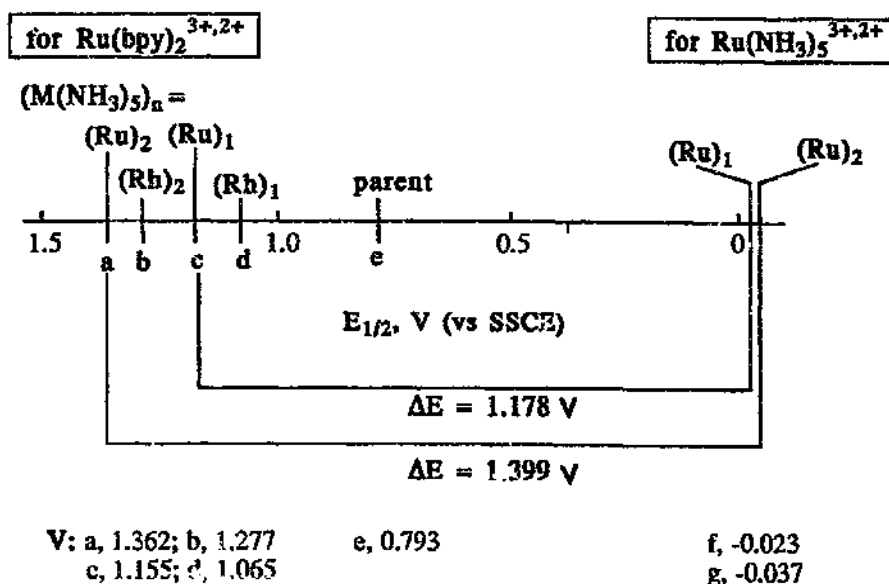


Fig. 5. Schematic diagram illustrating the contrasting electrochemical behavior of $\text{Ru}(\text{bpy})_2^{3+,2+}$ and $\text{Ru}(\text{NH}_3)_5^{3+,2+}$ couples in several $(\text{bpy})_2(\text{CN})_{2-n}\text{Ru}(\text{CNM}(\text{NH}_3)_5)_n^{3n+}$ complexes. Potentials determined in acetonitrile-TEAP solutions with an internal reference ($\text{Fe}(\text{Cp})_2^{0/+}$) and referenced to saturated calomel electrode (SCE).

As discussed below, values of $E_{1/2}^{\text{obsd}}$ for the $\text{Ru}(\text{NH}_3)_5^{3+,2+}$ probe couple in $\text{LM}(\text{CNRu}(\text{NH}_3)_5)$ complexes span a 350 mV range. This is about 250 mV more than expected based on the arguments sketched in Section 2, and it is more than 180 mV greater than expected based on these arguments and corrections to $E_{1/2}^{\text{ref}}$ discussed in the previous paragraph. A number of additional factors can be identified which probably contribute small amounts (ca. 20 mV) to this discrepancy, but the major problem appears to be in the application of Eqs. (1) and (5) to systems in which D-A coupling is very strong.

It should be apparent that the definition of $E_{1/2}^{\text{ref}}$ depends on the kind of information which one wishes to extract from ϵ_s^{th} . We would like ϵ_s^{th} to include all the contributions of $E_{1/2}^{\text{obsd}}$ which arise when D-A coupling is important. Since there is some mixing between LMCT, MLCT and DACT excited states of these molecules it is inevitable that some perturbational contributions of LMCT and/or MLCT states will contribute (differently) to both $E_{1/2}^{\text{ref}}$ and ϵ_s^{th} .

4.1.2. Contributions to ϵ_s^{th}

If we consider ϵ_s^{th} to contain only contributions which are correlated with the D-A coupling, then a major contributor will be ϵ_s^{op} as defined above. Other contribu-

tions will arise: (a) if other kinds of interactions (e.g. those involving LMCT and/or MLCT excited states of the bridging ligand) mix with the DACT excited states; (b) if other kinds of energies (e.g. zero-point energies of the bridging ligand); (c) from solvational effects which are associated with the partial charge delocalization which occurs when D–A coupling is significant (differential solvation effects). Examples and the significance of such contributions will be discussed below.

4.2. Systematic comparisons of D–A coupling inferred from spectroscopic and electrochemical measurements

We will focus our attention on some relatively recent studies. Earlier discussions of the issues involved can be found elsewhere [3,20,36,37].

4.2.1. Studies based on perturbational changes in non-bridging ligands

Curtis and co-workers have reported [14,15] some systematically correlated variations of $E_{1/2}^{\text{obsd}}$ with DACT oscillator strength. These were achieved by making small changes in the coordination sphere of D (or A), for example by varying substituents on L of a $\text{Ru}(\text{NH}_3)_4\text{L}$ moiety, and observing the electrochemical response of A in $\text{A}(\text{BL})\text{Ru}(\text{NH}_3)_4\text{L}$ (or of D in an analogous complex), where BL is an aromatic bridging ligand. These studies considered only the slopes of the resulting correlation lines, and $E_{1/2}^{\text{ref}}$ was considered to be unchanged through any one series. While there appear to be some uncompensated systematic changes in solvation energy (inferred from apparent changes in reorganizational energies) and in differential solvation through these series, these effects appear to be small, and this work strongly suggests that $\beta_{\text{BA}}^{\text{th}} > \beta_{\text{BA}}^{\text{sp}}$ for these systems.

4.2.2. Studies based on the variation of the coupled metals with ligands held constant

A different approach is to achieve the variations in D–A coupling by varying one of the metal centers while holding the bridging and non-bridging ligands constant. With this in mind, several series of $\text{LM}(\text{CN}^-)\text{Ru}(\text{NH}_3)_5$ complexes have been prepared and characterized [16,17,42–46]. Three of these series will be considered here: (a) $(\text{PP})_2(\text{CN})\text{M}(\text{CNRu}(\text{NH}_3)_5)^{3+}$ complexes in which $\text{PP} = \text{bpy}$ or phen and $\text{M} = \text{Fe}(\text{II})$, $\text{Ru}(\text{II})$, $\text{Rh}(\text{III})$ or $\text{Cr}(\text{III})$; (b) $(\text{PP})_2\text{M}(\text{CNRu}(\text{NH}_3)_5)_2^{n+}$ complexes for which $n=6$ when $\text{M} = \text{Fe}(\text{II})$ or $\text{Ru}(\text{II})$ and $n=5$ when $\text{M} = \text{Rh}(\text{III})$ or $\text{Cr}(\text{III})$; (c) $([\text{14}] \text{aneN}_4)\text{M}(\text{CNRu}(\text{NH}_3)_5)_2^{n+}$ complexes for $\text{M} = \text{Cr}(\text{III})$, $\text{Co}(\text{III})$ and $\text{Rh}(\text{III})$. Pertinent data are summarized in Table 2. Values of $E_{1/2}^{\text{obsd}}$ for these cyanoruthenates span a range of about 350 mV while values of ϵ_s^{sp} only span a range of about 70 mV (after taking account of different signs of ϵ_s^{th} for $\text{Cr}(\text{III})$ - and $\text{Ru}(\text{II})$ -centered complexes). This discrepancy is reasonably systematic, as is illustrated in Fig. 6. Fig. 6 contains three classes of complex: (a) $(\text{PP})_2\text{M}(\text{CNRu}(\text{NH}_3)_5)_2^{n+}$; (b) $(\text{PP})(\text{CN})\text{M}(\text{CNRu}(\text{NH}_3)_5)^{n+}$; (c) *trans*- $([\text{14}] \text{aneN}_4)\text{M}(\text{CNRu}(\text{NH}_3)_5)_2^{n+}$. The slopes of correlation lines are respectively 2, 4 and 0.9. However, it is important to observe that Fig. 6 is a plot of the raw experimental data, the observed value of $E_{1/2}$ for the $\text{Ru}(\text{NH}_3)_5^{3+,2+}$ couple and ϵ_s^{sp} based on the total oscillator strength of the lowest energy CT absorption band. That there are good correlations for each family of complexes, despite the several factors which are neglected in this figure, is

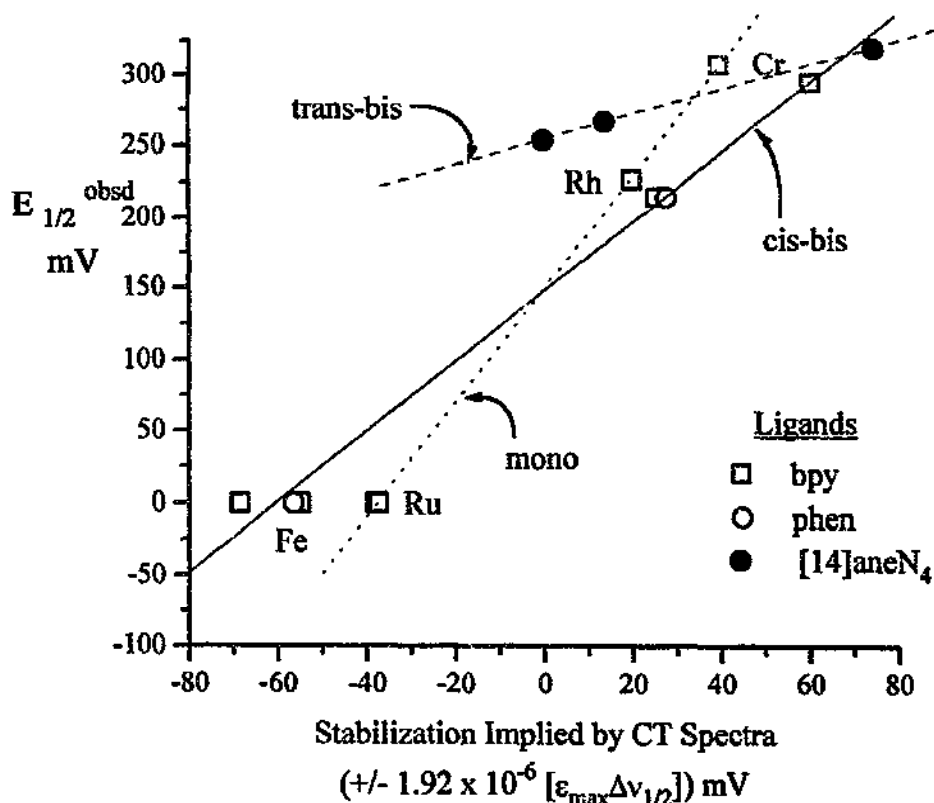


Fig. 6. Correlation of $E_{1/2}^{obsd}$ with the stabilization ϵ_s^{op} , implied by the lowest energy CT absorption band. The total observed oscillator strength was used for calculating $\epsilon_s^{op} = \pm 1.92 \times 10^{-6} (\epsilon_{max} \Delta\nu_{1/2})$; the donor–acceptor distance, across CN^- was taken to be 5.2 Å.

probably a consequence $\epsilon_s^{th} \gg \epsilon_s^{op}$. In order to generate a correlation which bears more definitively on the relationship between ϵ_s^{th} and ϵ_s^{op} , several corrections are necessary: (a) there is a large correction for symmetry effects, since the selection rules for light absorption and for the mixing of excited state and ground state wave functions are generally different in high symmetry complexes; (b) different charge transfer excited states can contribute to ground state stabilization, and these contributions may be different in different complexes; (c) there are probably small solvational differences from one complex to another (see preceding discussion); (d) there may be differences in zero-point vibrational energies resulting from the different charge distributions of the components of the redox couple. We will comment on the symmetry issues first, and the other points raised after the spectroscopy of these systems has been considered in a little more detail.

4.2.3. The role of symmetry in the comparison of ϵ_s^{th} and ϵ_s^{op}

If we consider sets of coplanar $d\pi(D)-d\pi(A)$ orbitals for $D(BL)A$ and $A(BL)D(BL)A$ complexes, then a simple symmetry argument can be employed to

Table 2
Comparison of cyanide stretching frequencies and DACT spectroscopic parameters in some cyanoruthenates

Complex ^a	ν_{CN}^b (cm^{-1})	DACT parameters ^c			$E_{1/2}^{\text{red d}}$ ((Ru(NH ₃) ₅) ^{3+,2+}) (V vs. SCE)	β_{DA}^e (cm^{-1} (per Ru))	$\epsilon_{\text{op f}}^f$ (cm^{-1})
		$\lambda_{\text{max}}^{\text{f}}$ (nm)	$\epsilon_{\text{max}}/10^3$ ($\text{cm}^{-1} \text{ M}^{-1}$)	$\Delta\nu_{1/2}/10^3$ (cm^{-1})			
Cr(III) centers							
Cr(bpy) ₂ (CN) ²⁺	2134 (w)						
(bpy) ₂ Cr(CN)(CNRu(NH ₃) ₅) ³⁺	2071, 2107(sh)	645	3.6	6.05	0.308	1924	338
(bpy) ₂ Cr(CNRu(NH ₃) ₅) ₂ ³⁺	2073	655	6.0	5.65	0.295	1955	525
trans-Cr(L ₁)(CN) ₂ ⁺	2090 (w)						
trans-Cr(L ₁)(CNRu(NH ₃) ₅) ₂ ³⁺	2076	500	8.00	4.90	0.320	1870	608
cis-Cr(L ₂)(CN) ₂ ⁺	2132 (w)						
cis-Cr(L ₂)(CN)(CNRu(NH ₃) ₅) ₂ ³⁺	2077	530	3.2	5.00		1964	248
cis-Cr(L ₂)(CNRu(NH ₃) ₅) ₂ ³⁺	2070	522	8.00	5.10	0.320	2160	632
Ru(II) centers							
Ru(bpy) ₂ (CN) ₂	2060, 2072 (s)						
(bpy) ₂ Ru(CN)(CNRu(NH ₃) ₅) ³⁺	2019, 2075	700	4.45	4.50	-0.023	1766	311
(bpy) ₂ Ru(CNRu(NH ₃) ₅) ₂ ⁶⁺	2011, 2057	655	7.77	5.00	-0.037	1834	602
(bpy) ₂ Ru(CNRu(NH ₃) ₅)(CNRu(NH ₃) ₅) ⁶⁺	2019, 2121	670	~5.4 ^g	5.28	-0.004	~2 × 10 ³	
(bpy) ₂ Ru(CN)(CNRu(NH ₃) ₅) ³⁺	2062, 2105 ^h						
(bpy) ₂ Ru(CNRu(NH ₃) ₅) ₂ ⁶⁺	2105, 2124 ^h						
(bpy) ₂ Ru(CNRu(NH ₃) ₅) ₂ ⁶⁺	2090, 2130 ^h						
Ru(tpy)(bpy)(CN) ⁺	2076(5)	700	4.10	4.90	0.045	1774	312
(tpy)(bpy)Ru(CNRu(NH ₃) ₅) ⁴⁺	2020						
Fe(II) centers							
Fe(bpy) ₂ (CN) ₂	2070, 2078 (s)						
(bpy) ₂ Fe(CNRu(NH ₃) ₅) ₂ ⁴⁺	2091, 2081						
(bpy) ₂ Fe(CNRu(NH ₃) ₅) ₂ ⁴⁺	2033, 2019	875	6.58	4.75	0.000	1388	484
(bpy) ₂ Fe(CNRu(NH ₃) ₅) ₂ ⁴⁺	2065, 2079 (s)						
Fe(Phen) ₂ (CN) ₂	~2080						
(phen) ₂ Fe(CNRu(NH ₃) ₅) ₂ ⁴⁺	~2025	880	6.80	4.75	0.000	1400	501
(phen) ₂ Fe(CNRu(NH ₃) ₅) ₂ ⁴⁺							

Table 2 (continued)

Rh(III) centers							
Rh(bpy) ₃ (CN) ²⁺	2141, 2148 (s)						
(bpy) ₃ Rh(CN)(CN)(Ru(NH ₃) ₃) ³⁺	2143						
(bpy) ₃ Rh(CN)Ru(NH ₃) ₃ ⁵⁺	2140	— ^{j,j}	0.227	~0 ^j			
Rh(phen) ₂ (CN) ²⁺	2144	— ^{j,j}	0.215	~0 ^j			
(phen) ₂ Rh(CN)Ru(NH ₃) ₃ ⁵⁺	2140		0.215	~0 ^b			
trans-Rh(L ₁)(CN) ²⁺	2126						
trans-Rh(L ₁)(CNRu(NH ₃) ₃) ²⁺	2110	1	0.254	~0			
Co(III) centers							
trans-Co(L ₁)(CN) ²⁺	2130						
trans-Co(L ₁)(CNRu(NH ₃) ₃) ²⁺	2110	501	1.03	7.01	1060	112	

^a Macrocyclic ligands: [20] L₁ = [14]aneN₄(cyclam); L₂ = *rac*-Me₆[14]aneN₄; see Fig. 4. ^b w, weak; s, strong; no designation implies medium; sh = shoulder.
^c Parameters from Refs. [16–19]. ^d In acetonitrile-TEAP with Fe(Cp)₂ as internal reference. ^e β_{DA} calculated iteratively from Eqs. (5) and (6) using data in this table. ^f $\epsilon_{\text{CT}}^{\text{CT}} = (\beta_{DA}^{\text{CT}})^2/E_{\text{CT}}$, where β_{DA}^{CT} is the energy of the observed DACT absorption maximum, ϵ_{max} and $\Delta\epsilon_{1/2}$ are the observed absorptivity and bandwidths. ^g By weight of salt; absorption in acetonitrile. All others from redox titrations in water. ^h Refs. [18,43]. ⁱ Lowest energy transition is assigned as Ru(NH₃)₃²⁺ → bpy (or phen) CT. No DACT absorption is observed (see Refs. [45,46]. ^j Ref. [43]. ^k Refs. [19,42]. ^l Refs. [16,19]; lowest energy transition assigned as Ru(NH₃)₃²⁺ → CN⁻ (π^*).

show that [47]: (a) excitation to the DACT excited state of D(BL)A is dipole allowed with an absorption intensity of I_A ; (b) in *cis*-A(BL)D(BL)A, with an effective C_2 symmetry, the DACT excited states have A and B symmetry; optical transitions to both of them are dipole allowed, but only one is the symmetry appropriate for mixing with the ground state (if the A and B transitions are convoluted within the same absorption envelope, as in the CN^- -bridged complexes, then the total absorption intensity would be $2I_A$); (c) in *trans*-A(BL)D(BL)A complexes a dipole allowed transition is expected for one of the two DACT excited states (the 'ungerade' state) while the other has the symmetry appropriate for mixing with the ground state (the weighted absorption intensity would be $2I_A$). In an actual detailed comparison of ϵ_s^{th} and ϵ_s^{op} it is necessary to make some assumptions about the intensities of the various symmetry allowed transitions [26,47]. Parker and Crosby [47] have assumed, in treating metal complexes with polypyridyl acceptors, that the intensities of the z -allowed components far exceed those of the x,y -allowed components, and this assumption is consistent with the observed polarizations [48]. However, even for the Creutz-Taube ion, $[Ru(NH_3)_5]_2pz^{5+}$, there appears to be considerable intensity in the y -component of the DACT absorption [49]. The CN^- -bridged complexes have roughly cylindrical symmetry along the bridging axis and there is no obvious physical basis for assuming that 'local dipoles' [26] are of negligible magnitude in the x,y -plane; therefore, we have included the complete set of $d\pi(D)$ and $d\pi(A)$ symmetry terms in our analysis. It is important to observe that the DACT intensities of the bis-ruthenates (*cis*- and *trans*-) are always almost twice those of the corresponding mono-ruthenates, so that the Parker and Crosby extension of the Mulliken argument about the rules of symmetry and local transition dipole contributions should still be nearly correct. For example, if one assumes that the various symmetry components are nearly equally weighted and assuming C_{2v} symmetry we would predict a ratio of intensities for *cis*-bis- to *cis*-mono-ruthenates of 1.6/1 and for $RuCNRu$ systems we observe 1.7/1 [42]; C_2 symmetry would lead to the 2/1 ratio of Parker and Crosby. Owing to their 4A_2 ground states, the $Cr(III)$ -centered complexes are a little more complicated, but the intensity ratios are similar for the *cis*-bis- to *cis*-mono-ruthenate intensities, while a somewhat smaller ratio (1.4/1) would result for the *trans*-bis-ruthenates if all the intensity components were equally weighted.

While the transition dipole operator has x,y and z -type symmetry components, only one symmetry type (not generally corresponding to a dipole symmetry species) will mix with the ground state. Thus, one generally expects differences in the numbers and symmetry types of DACT components which contribute to the absorption intensity and to the ground state stabilization. In the mono-ruthenates one expects a 1/1 correspondence [26,47], but in the *cis*- $Ru^{II}(CNRu^{III})_2$ complexes the ratio of components which could contribute to intensity to those contributing to ground state stabilization (averaged over possible ground state configurations) is 2.8/1 for C_{2v} and 2/1 for C_2 symmetry [42]. For *cis*- $Cr^{III}(CNRu^{II})_2$ these ratios are 3/1 and 2/1 respectively, and for *trans*- $Cr^{III}(CNRu^{II})_2$ the ratio is 3/1 for D_{3h} and 2/1 for D_{2h} symmetry. The last of these differs from the example presented by Parker and Crosby [47] because we have included x,y components in the transition intensity.

However, this result is in agreement with the similarity of values for $E_{1/2}^{\text{obsd}}$ and ϵ_s^{op} found for *trans*-([14]aneN₄)Cr(CNRu(NH₃)₅)₂⁵⁺ and for *cis*-(*rac*-Me₆[14]aneN₄)Cr(CNRu(NH₃)₅)₂⁵⁺ (Table 2).

The net result of these symmetry considerations is that, in the simplest limit of equally weighted DACT components, the value of ϵ_s^{op} to be used in the correlations with $E_{1/2}^{\text{obsd}}$ must be corrected so that these quantities contain the same number of contributing DACT components. A reasonably conservative approach is to divide the apparent value of ϵ_s^{op} based on the total oscillator strength of the DACT absorption (as in the values in Table 2) by two for the bis-ruthenates. This correction will make the correlation lines for *cis*-(bpy)₂M(CNRu(NH₃)₅)₂⁵⁺ and (bpy)₂(CN)Ru(CNRu(NH₃)₅)₂⁵⁺ nearly coincident with a slope of about 4.2, and it will increase the slope of the correlation for the *trans*-([14]aneN₄)M(CNRu(NH₃)₅)₂⁵⁺ complexes to about 2.

4.2.4. Red shift of the cyanide stretching frequencies in CN[−]-bridged D–A complexes

The CN[−] stretching frequency turns out to be relatively sensitive to the electronic properties of the coordinated metals. Thus ν_{CN} is usually in the range of 2125–2150 cm^{−1} for most mono- and bis-cyano metal complexes (e.g. for complexes of Cr(III), Rh(III), Co(III), Pt(II), see Ref. [18] and Table 2). However, when the metal is relatively ionizable (e.g. for Ru(II), Fe(II); see Table 2) ν_{CN} tends to be shifted to lower energy (2060–2080 cm^{−1} in the examples cited), and this can be attributed to ‘back bonding’, or, more systematically, to the delocalization of electron density through MLCT. When the CN[−] acts as a bridging ligand between two metals, ν_{CN} shifts to higher frequency [49] unless the two metals form a donor-acceptor pair [18]. When this is the case, ν_{CN} shifts to even lower energy (Table 2). The shift, relative to the monometal parent, of ν_{CN} in the bridged D–A complexes is roughly proportional to the D–A coupling matrix element, β_{DA} , Fig. 7. These observations suggest that the D–A coupling and the CN[−] stretch are themselves coupled.

4.2.5. Charge-transfer spectroscopy of the CN[−]-bridged complexes: coupling and mixing of chromophores

There are several absorption bands of the CN[−]-bridged complexes which depend on the oxidation state of the Ru(NH₃)₅ moiety. There is a great deal of mixing and ‘intensity stealing’ between these states and with other CT states of these molecules. This is illustrated in Fig. 8, which shows the absorption changes which accompany the Fe²⁺ oxidation of (bpy)₂Ru(CNRu(NH₃)₅)₂⁴⁺. The DACT absorption bands are labeled (a) in this figure. The higher energy absorptions of the Ru(CNRu)₂ complex are readily assigned, in the order of increasing energies, Ru(NH₃)₅²⁺ → bpy MLCT ((c) at about 480 nm), central Ru²⁺ → bpy MLCT ((b) at about 400 nm), Ru(NH₃)₅²⁺ → CN[−] MLCT ((f) at about 380 nm) and CN[−] → Ru(NH₃)₅²⁺ LMCT ((e) at about 350 nm). These transitions have been identified by comparison of many complexes, including especially the macrocyclic ligand complexes in which there can be no M → bpy MLCT transitions. For the (bpy)₂Fe(CNRu(NH₃)₅)₂⁴⁺ complex the Fe²⁺ → bpy MLCT transition shifts to an

Dependence of ν_{CN} Red Shift on Donor-Acceptor Coupling

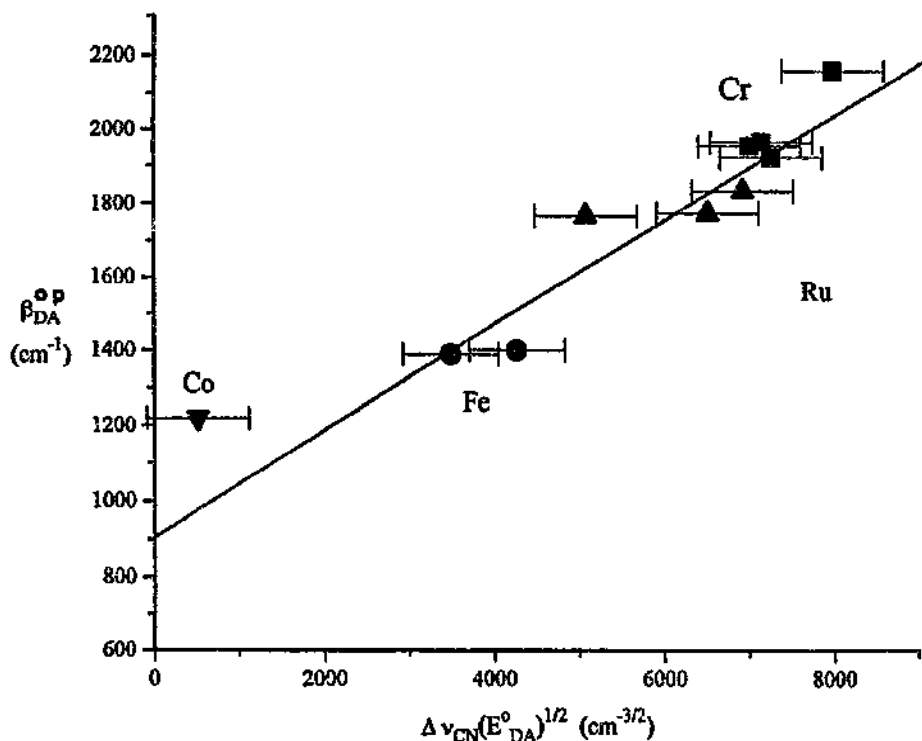


Fig. 7. Correlation of the shifts of ν_{CN} to lower frequencies in D-A complexes with the D-A coupling inferred from the DACT absorption spectra. The point for $(\text{bpy})_2\text{Co}(\text{CN})\text{CNKu}(\text{NH}_3)_5^{3+}$ has been corrected for the expected smaller oscillator strength of the $d\pi-d\sigma$ system than the $d\pi-d\pi$ systems (see Table 2).

energy comparable with, or somewhat lower, than that of the $\text{Ru}(\text{NH}_3)_5^{2+} \rightarrow \text{bpy}$ transition, and the mixing between these MLCT states appears to result in an even lower energy for the $\text{Fe}^{2+} \rightarrow \text{bpy}$ MLCT transition in this than in the parent complex. The $\text{Ru}(\text{NH}_3)_5^{2+} \rightarrow \text{bpy}$ MLCT absorbance can be identified in all the $(\text{bpy})_2\text{M}(\text{CN})_2^{n+}$ mono- and bis-ruthenates, and it always appears to consist of two components separated by about $4 \times 10^3 \text{ cm}^{-1}$. These transitions vary a great deal in their oscillator strengths as a result of the mixing with $\text{M}^{2+} \rightarrow \text{bpy}$ MLCT or with the DACT states. These spectroscopic effects of the mixing between various CT states can be interpreted as experimental measures of the delocalized nature of the wave functions of these states, and there are some resulting ambiguities about the choice of experimental parameters used in evaluating ϵ^{op}_1 . In a first-order perturbation theory argument the parameters to be used refer to the unperturbed, or diabatic states [26]. At this level of argument the stabilization of $\text{Ru}(\text{NH}_3)_5^{2+}$ which derives

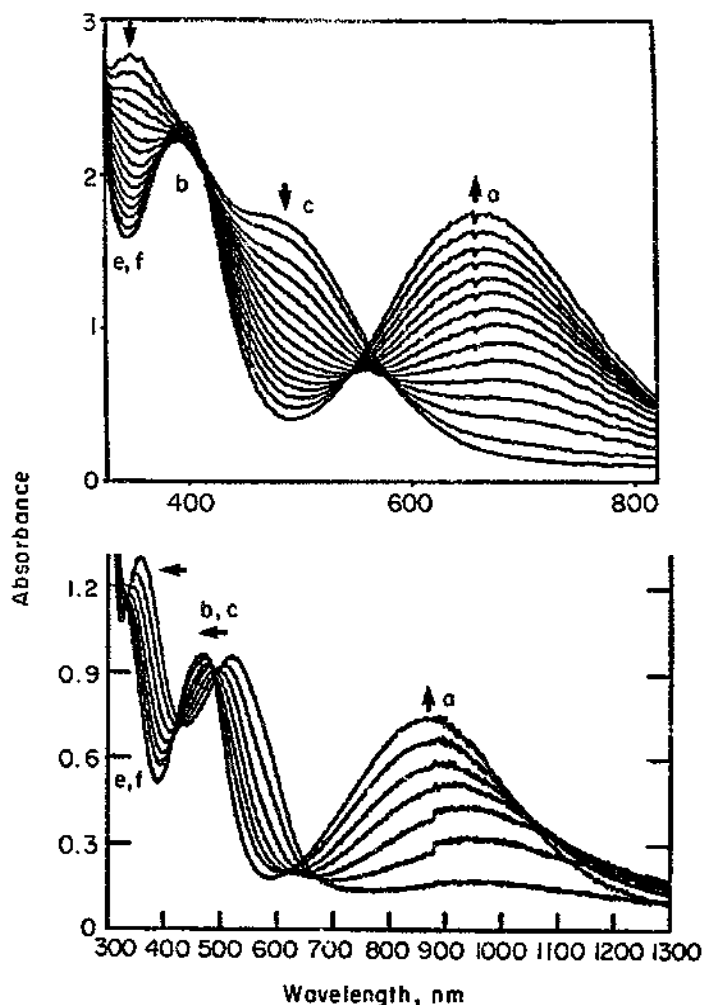


Fig. 8. Spectroscopic changes which accompany the oxidation of $(bpy)M(CNRu(NH_3)_5)_2^{2+}$ complexes with Fe^{2+} (aq.): $M=Ru(II)$, top; $Fe(II)$, bottom. Absorption bands are assigned as: DACT, (a); $M \rightarrow bpy$ MLCT, (b); $Ru(NH_3)_5^{2+} \rightarrow bpy$ MLCT, (c); $CN^- \rightarrow Ru(NH_3)_5^{2+}$ LMCT, (e); $Ru(NH_3)_5^{2+} \rightarrow CN^-$ MLCT, (f).

from mixing with the $Ru(NH_3)_5^{2+} \rightarrow bpy$ MLCT state would be the same through the series of complexes, and this will not contribute to the slopes in Fig. 5. Variations in the higher-order terms could make a contribution. A very rough estimate suggests about 10 mV greater contribution to $E_{1/2}^{obsd}$ from higher-order terms in the $Cr(III)$ - and $Fe(II)$ - than in the $Ru(II)$ -centered complexes; however, these higher-order CT mixings do not occur in the $Rh(III)$ -centered complexes, and taking them into account would suggest an even larger difference in values of $E_{1/2}^{obsd}$ for these complexes and those with $Ru(II)$ or $Fe(II)$ centers (by 10–30 mV). We will neglect these

second-order effects. Similar issues arise in regard to $\text{Ru}(\text{NH}_3)_5\text{CN}^-$ MLCT and LMCT excited states, and this mixing is a feature of the vibronic argument below.

4.2.6. Variations in the solvational contributions of $E_{1/2}^{\text{obsd}}$

Two kinds of solvational interaction need to be considered: (a) the solvational contributions, ΔG_s^\ominus , to $E_{1/2}^{\text{ref}}$ for the particular class of complexes (here for complexes which have the same ligands and charge type); (b) the correction to ΔG_s^\ominus which arises from the charge delocalization associated with D–A (differential solvation correction), $\delta\Delta G_s^\ominus$. The first of these was discussed in Section 4.1.1.

If the donor and acceptor are solvated differently, as is certainly the case for the ruthenates of $\text{M}(\text{PP})(\text{CN})_2^{2+}$, then the changes of charge distribution induced by D–A coupling will alter the value of ΔG_s^\ominus . This effect can be analyzed in terms of the simple electrostatic model for the solvation. Thus, the effective charge at the redox site is increased by an amount α_{DA}^2 if Ru(II) is stabilized. Assuming (for purposes of a maximum correction) that the charge density is mostly localized on $\text{Ru}(\text{NH}_3)_5$, and after some algebraic manipulations, the corrections arising from the differential solvation effects for D–A stabilization of Ru(II) and Ru(III) can respectively be evaluated as in Eqs. (9) and (10) [19,42]. Since ΔG_s^\ominus is not readily available, we will assume that

$$(\delta\Delta G_s^\ominus)_{\text{II}} \approx -\varepsilon_s^{\text{op}} \Delta G_s^\ominus / E_{\text{DA}} \quad (9)$$

$$(\delta\Delta G_s^\ominus)_{\text{III}} \approx -0.66\varepsilon_s^{\text{op}} \Delta G_s^\ominus / E_{\text{DA}} \quad (10)$$

$\Delta G_s^\ominus \approx \lambda_{\text{reorg},s}$, where $\lambda_{\text{reorg},s}$ refers to the solvent reorganizational contribution for D→A electron transfer. This approximation works well with Richardson's estimates of ΔG_s^\ominus for the $\text{Ru}(\text{bpy})_2^{3+,2+}$ and $\text{Ru}(\text{NH}_3)_5^{3+,2+}$ couples [39] and the reorganizational energy differences of the respective self-exchange electron transfer reactions. For the $d\pi$ – $d\pi$ DACT transitions of the $(\text{bpy})_2\text{M}(\text{CNRu}(\text{NH}_3)_5)_2^+$ complexes, $\lambda_{\text{reorg},s} \approx 3.5 \times 10^3 \text{ cm}^{-1}$ (based on fits to Eqs. (3) and (6)). This effect will always tend to increase $E_{1/2}^{\text{obsd}}$ in these systems, and we estimate that the maximum amount of this increase is about 12 mV. Obviously there will be no contributions from this source if $\varepsilon_s^{\text{op}} \approx 0$ (as for Rh(III)-centered complexes).

4.2.7. Spin multiplicity contributions and other effects of M–M' coupling

Contributions to $E_{1/2}^{\text{obsd}}$ which result from M–M' coupling in the fully oxidized (A(BL)A') or fully reduced (D(BL)D') complexes must also be taken into account. These will generally be a combination of enthalpic (arising from coupling energies) and entropic (arising from multiplicity changes) contributions. In the complexes considered here, interactions of this type are of concern for Cr(III)–Ru(III), Ru(III)–Ru(III) and for Fe(III)–Ru(III) complexes. For example, a smaller than expected value of $E_{1/2}^{\text{obsd}}$ would result if spin–spin coupling in these complexes was largely ferromagnetic. This effect could result in a smaller difference between $E_{1/2}^{\text{obsd}}$ for $(\text{bpy})_2\text{Cr}(\text{CNRu}(\text{NH}_3)_5)_2^{5+,7+}$ and the $(\text{bpy})_2\text{Rh}(\text{CNRu}(\text{NH}_3)_5)_2^{5+,7+}$ 'reference' than is found for the Ru(II)- or Fe(II)-centered analogs. This point has also been raised in regard to the comparison between Ru(II)–Ru(II)/Ru(III)–Ru(III) and

Ru(II)–Ru(II)/Ru(II)–Ru(II) couples [17]. A three-center perturbational coupling, $D^+ - \pi(CN^-) - A$, in the oxidized complexes could be consistent with a ferromagnetic interaction.

We also note that weak antiferromagnetic coupling could result in somewhat larger values of $E_{1/2}^{obsd}$. This possibility seems somewhat less consistent with observations on the CN^- -bridged complexes.

We hope to resolve the ambiguity regarding the magnetic correction in the near future. For purposes of the present discussion we will postulate a total (enthalpic plus entropic) contribution of about -60 mV to $E_{1/2}^{obsd}$ in the Cr(III)-centered complexes.

4.2.8. Changes in vibrational frequencies and zero-point energy differences

The contributions of vibrational frequency differences of components of a redox couple on values of $E_{1/2}^{obsd}$ have been discussed by Richardson and Sharp [38]. Since we have used a constant probe couple in Fig. 6, the only frequency change of concern here is that of the bridging CN^- . The zero-point energy differences are easily evaluated from the data in Table 2, and these will contribute from $+8$ mV (for $Cr(CNRu)_2$ complexes) to -10 mV (for $Ru(CNRu)_2$ complexes) to $E_{1/2}^{obsd}$.

4.3. The effect of estimated correction terms on the correlation of $E_{1/2}^{obsd}$ with ϵ_s^{op}

The net effect of the corrections described above is to slightly increase the ratio of $\epsilon_s^{th}/\epsilon_s^{op}$ for the $M(PP)_2$ -centered complexes, and they result in essentially the same ratios (i.e. 4–5 and ≈ 2) of $\epsilon_s^{th}/\epsilon_s^{op}$ for the $M(PP)_2$ - and $M([14]aneN_4)$ -centered complexes. These corrections do result in a value of $(E_{1/2}^{obsd})_{corr}$ for the $Rh(PP)_2$ -centered complexes which is near to the average of those for the $Cr(PP)_2$ and $Ru(PP)_2$ analogs, in reasonable accord with expectation for a 'reference' system. While these corrections are each quite plausible, the uncertainties of the larger correction terms are quite large, and no particular significance can be attached to the numerical magnitude of the ratio of $\epsilon_s^{th}/\epsilon_s^{op}$ at this time. However, the important qualitative result is that ϵ_s^{th} is significantly larger than ϵ_s^{op} in these systems. This result strongly supports those of our initial reports [16,17] that $\epsilon_s^{th} \geq 2\epsilon_s^{op}$, which was based mostly on the comparison $E_{1/2}^{obsd}$ (for $Ru(bpy)_2^{3+,2+}$) and ϵ_s^{op} : (a) $(bpy)_2Ru(CNRu(NH_3)_5)^{6+}$ relative to $(bpy)_2Ru(CNRh(NH_3)_5)^{6+}$; (b) $(bpy)_2Ru(CNRu(NH_3)_5)^{6+}$ relative to $(bpy)_2Ru(CNRu(NH_3)_5)(CNRh(NH_3)_5)^{6+}$; (c) $(bpy)_2(CN)Ru(CNRu(NH_3)_5)^{3+}$ relative to $(bpy)_2(CN)Ru(CNRh(NH_3)_5)^{3+}$. We note that $E_{1/2}^{obsd}$ for all the $RuCNRu$ complexes in these earlier comparisons are subject to a correction for M–M' coupling, in the paramagnetic $Ru(III)$ – $Ru'(III)$ complexes, which would probably have the effect of increasing the $\epsilon_s^{th}/\epsilon_s^{op}$ ratio.

4.4. Summary: some experimental consequences of strong D–A coupling

For a wide range of experiments on strongly coupled D–A complexes, reviewed above, the observations are not readily accommodated by crude Born–Oppenheimer-based perturbation theory models. Yet some other aspects of the observed

experimental behavior do, at least qualitatively, fit with expectation for CT-perturbed chemistry.

In studies of fast BET processes in CN^- -bridged D–A complexes, it has been shown that the crossing between ‘states’ with different electronic configurations appears to occur more rapidly than vibrational relaxation within a single electronic configurational manifold. This behavior cannot be described in terms of simple potential energy surfaces for the electronic excited states, and it suggests that the Born–Oppenheimer approximation may not be very useful in such systems.

Ground state spectroscopic studies indicate that there is considerable mixing between various chromophores. Probably the most important behavior of this type is the observed coupling between the bridging CN^- stretching frequency and the oscillator strength of the DACT absorption. This clearly demonstrates that the CN^- stretch and the electronic coupling between donor and acceptor cannot be treated separately. Thus, at least with respect to this coupling, the crude Born–Oppenheimer approximations cannot be useful.

Finally, the variations in ground state redox properties of D–A complexes correlate strongly with the DACT absorption oscillator strength, as expected from simple perturbation theory arguments, but the magnitude of the ground state stabilization is larger than predicted by Born–Oppenheimer-based perturbation theory arguments.

These observations suggest that the perturbational mixing of CT excited states with the ground state should be treated by allowing for some coupling of the nuclear and electronic coordinates. This is analogous to the nuclear–electronic coupling which arises in Jahn–Teller and pseudo-Jahn–Teller problems [50–52]. A simple vibronic argument is developed below which is at least qualitatively consistent with the observations.

5. A simple vibronic approach to D–A coupling

Vibronic approaches to electron transfer systems have been discussed in general terms [53,54], with respect to the spectroscopy of the Creutz–Taube ion [55,56] and with respect to proton-coupled electron transfer systems [57,58]. Our concern in trying to treat the systems described in this paper was to find a model which was conceptually simple, but which could still be used to interrelate several different kinds of experimental observation. A further consideration was to develop an argument in which all the parameters were either directly measurable or easily interpolated from measured parameters. A key element in our approach is the observation that the $\text{CN}^- \rightarrow \text{Ru(III)}$ and the $\text{Ru(II)} \rightarrow \text{CN}^-$ LMCT and MLCT transitions are of roughly comparable intensity and occur in roughly the same spectroscopic region [59–63], and that the combination of an $\text{M(II)} \rightarrow \text{CN}^-$ MLCT combined with a $\text{CN}^- \rightarrow \text{M'(III)}$ LMCT across a bridging ligand will result in some net delocalization of electron density from donor to acceptor, even if there is no direct D–A coupling. In such a system, $\text{M(II)} \rightarrow \text{CN}^-$, $\text{CN}^- \rightarrow \text{M'(III)}$ and $\text{M(II)} \rightarrow \text{M'(III)}$ CT interactions will be coupled. If we focus on these interactions, and if we treat the LMCT, MLCT and DACT interactions stepwise, then we may

first consider the LMCT and MLCT perturbational stabilizations of the ground state (through stabilization energy terms, as in Section 2, added to the diabatic potential function for the ground state V_D^0) and the generally numerically different LMCT and MLCT stabilizations of the electron transfer excited state (through stabilization terms added to the diabatic potential V_A^0). If we label the electron transfer coordinate as x , and average the LMCT and MLCT contributions for simplicity, then the resulting stabilization energies, ϵ_{CT} and ϵ'_{CT} , may be expanded in Taylor's series around x , and if we ignore second- and higher-order terms in this expansion (i.e. $\epsilon_{CT} \approx \epsilon_{CT}^0 + ax$, etc.), then the resulting potential functions are given by Eq. (11) and Eq. (12)

$$V_D = V_D^0 + kx^2/2 + ax \quad (11)$$

$$V_A = V_A^0 + k'x^2/2 + a'x \quad (12)$$

where k and k' are force constants associated with the respective diabatic surfaces, $V_i' = V_i^0 \pm \epsilon_{CT}^0 + kr_o^2/2$ and $a' \approx a - kr_o + \alpha_{CT}^2 kr_o$. If the D–A coupling is also a linear function of displacement along x (as for example for very small displacements and an exponential distance dependence of β_{DA}), then $\beta_{DA} = \beta_{DA}^0 + bx$ where β_{DA}^0 refers to the coupling when $x=0$. If we assume for algebraic simplicity that $a \approx a'$, then the resulting second-order secular equation can be readily solved for the potential energy of the coupled system; for small displacements the solutions are of the form given in Eq. (13)

$$V_{\pm} = kx^2/2 + E_{DA}'/2 \pm 1/2 [E_{DA}'^2 + 4axE_{DA}' + 4a^2x^2 + 4(\beta_{DA}^0 + bx)^2]^{1/2} \quad (13)$$

where $E_{DA}' = V_{DA}' - V_D^0$ is assumed to be large; V_- represents the ground state potential energy surface after vibronic coupling. The qualitative effects of this vibronic perturbation are illustrated in Fig. 9 and can be summarized: (a) the potential energy minima, of V_+ and V_- , are displaced along the coordinate x from those of the diabatic, V_A^0 and V_D^0 , or the CT-perturbed, V_A' and V_D' , potential energy surfaces; (b) the ground state potential energy surface V_- is 'flatter' than the diabatic surface; (c) the separation of the electron transfer ground and excited states is increased, relative to that of either the diabatic or CT-perturbed surfaces, and characteristic of an adiabatic reaction; (d) the displacement of potential energy surfaces along x alters the contribution to the ground state stabilization which arises from the CT perturbation (this D–A-induced variation in ϵ_{CT} is ax_{min}).

The amplitude of the displacement of the ground state potential energy surface can be evaluated from dV/dx , and is given to a reasonable level of approximation by Eq. (14)

$$x_{min} \approx (a + 2\alpha_{DA}^0 b)/k \quad (14)$$

where $\alpha_{DA}^0 = \beta_{DA}^0/E_{DA}'$. The linear vibronic parameters a and b can be evaluated from the consideration of limiting cases [18,19,42] or from their relation to the Huang–Rhees, parameter of spectroscopic arguments [52]; thus, $a \approx 4\alpha_{CT}^0(\lambda_{CT}k_{CT}/2)^{1/2}$ and $b \approx (\lambda_{DA}k_{DA}^2)^{1/2}$, where $\alpha_{CT}^0 = \beta_{CT}^0/E_{CT}^0$ (average of LMCT

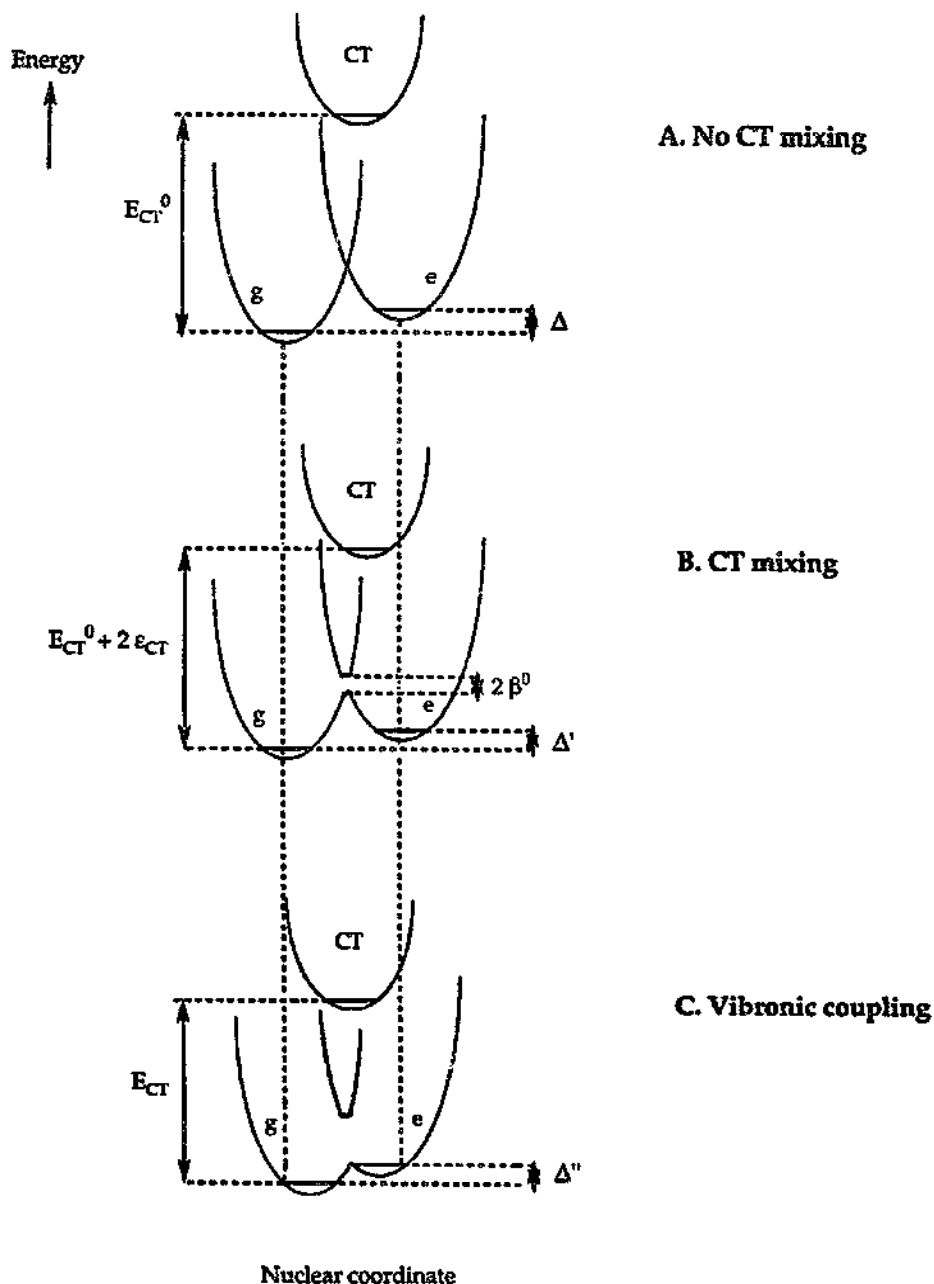


Fig. 9. Qualitative potential energy surfaces illustrating the effects of the successive perturbations employed in the simple vibronic model: diabatic surfaces, (A); LMCT and MLCT (averaged) mixing with the ground and excited electron transfer states ((g) and (e)), (B); and the result of vibronic D-A coupling, (C).

and MLCT), the λ_i are the respective nuclear reorganizational parameters for the electron transfer process indicated and the k_i are the respective force constants (for simplicity, we assume all force constants are equal, $k_i = k$).

Similarly, the effective force constant for the ground state surface can be evaluated from $d^2V/dx^2 = k_{\text{eff}}$ and the difference between k_{eff} and the force constant k , for the diabatic surfaces is a measure of the flattening of V_- . From Eq. (13), we can obtain Eq. (15).

$$k_{\text{eff}} \approx k - 2(a^2 + b^2)/E_{\text{DA}}^{\ominus} \quad (15)$$

Since $\beta_{\text{DA}} = (\beta_{\text{DA}}^{\ominus} + bx_{\text{min}})$ also varies with the parameters a and b , one can readily infer similar trends in the variations of v_{eff} and β_{DA} ; if v_{eff} is proportional to v_{CN} (or $\Delta v_{\text{eff}} \approx \gamma \Delta v_{\text{CN}}$) then the approximate relationship in Eq. (16) can be obtained [42].

$$\beta_{\text{DA}} \approx \beta_{\text{DA}}^{\ominus} + 2\gamma(\Delta v_{\text{CN}}/v_{\text{eff}})\beta_{\text{DA}}^{\ominus} + \dots \quad (16)$$

This expression accounts for the correlation in Fig. 6. The difference between V_{D} and V_- is the effective ground state stabilization which results from vibronic coupling between a DACT excited state and the ground state. This difference is most simply represented as in Eq. (17)

$$(\varepsilon_s^{\text{th}})_v \approx (\beta_{\text{DA}}^{\ominus})^2/E_{\text{DA}}^{\ominus} + k(x_{\text{min}})^2/2 + (a^2 + b^2)x_{\text{min}}^2/E_{\text{DA}}^{\ominus} \quad (17)$$

where the first term is the stabilization energy obtained from the perturbational approach outlined in Section 2. In terms of the same perturbations, $\varepsilon_s^{\text{op}}$ is given by Eq. (18).

$$(\varepsilon_s^{\text{op}})_v \approx (\beta_{\text{DA}}^{\ominus} + bx_{\text{min}})^2/E_{\text{DA}}^{\ominus} \quad (18)$$

In terms of the electron transfer parameters, introduced above, the difference in these quantities is given by Eq. (19) in the limit that $\lambda_{\text{DA}} < E_{\text{DA}}^{\ominus}$, which is always correct for the systems discussed here.

$$(\varepsilon_s^{\text{th}})_v - (\varepsilon_s^{\text{op}})_v \approx 4(\alpha_{\text{CT}}^{\ominus})^2\lambda_{\text{CT}} - 2(\alpha_{\text{DA}}^{\ominus})^2\lambda_{\text{DA}} \quad (19)$$

In the model used here, $\alpha_{\text{DA}}^{\ominus} < \alpha_{\text{CT}}^{\ominus}$ (D–A coupling mediated by local CT interactions) and $\lambda_{\text{DA}} < \lambda_{\text{CT}}$ for the CN^- -bridged systems considered here, so Eq. (19) is qualitatively consistent with the experimental observations that $\varepsilon_s^{\text{th}} > \varepsilon_s^{\text{op}}$. A very rough estimate, based on spectroscopic observations mentioned above, indicates that the difference predicted by Eq. (19) is greater than 35 mV, and is thus comparable with $\varepsilon_s^{\text{op}}$ (for RuCNRu systems, using LMCT and MLCT parameters from *trans*-([14]aneN₄)Rh(CNRu(NH₃)₅)₂⁵⁺). A more critical evaluation will depend on deconvolution of the MLCT and LMCT absorptions in the D–A complexes, but it appears that intensity stealing results in increases of these absorptions in many of the complexes. It should be noted that cross-terms $(\alpha_{\text{DA}}^{\ominus}\alpha_{\text{CT}}^{\ominus}[\lambda_{\text{CT}}\lambda_{\text{DA}}]^{1/2})$ which arise in Eq. (17) and Eq. (18) can be interpreted to be the consequence of mixing between DACT, MLCT and LMCT excited states. Thus, the model described here attributes the observation that $\varepsilon_s^{\text{th}} > \varepsilon_s^{\text{op}}$ to enhanced MLCT and LMCT couplings which arise as a result of the synergistic D–A coupling.

6. Summary and conclusions

The observations summarized above indicate that a simple vibronic perturbation, in place of the usual Born–Oppenheimer-based electronic perturbation, can, at least qualitatively, account for several aspects of the otherwise anomalous behavior of strongly coupled D–A systems. A more critical evaluation of the implications of the vibronic model will depend on deconvolution of the MLCT and LMCT absorptions in the actual D–A complexes, since any variations in oscillator strength, such as result from mixing with other kinds of excited state, will be very important. For the present, even qualitative agreement is encouraging.

6.1. Some implications of vibronic coupling

The possibility, which is argued in this paper, that strong D–A coupling involves a mixture of nuclear and electronic components raises several additional issues which need to be investigated. Thus, if the D–A coupling in these systems is predominantly bridging-ligand-mediated, and if β_{DA} is indeed a function of the electron transfer coordinate, then β_{DA} determined from the optical absorption (for which $x = x_{min}$) is not appropriate for evaluation of rate constants (k_{BET}) at the electron transfer transition state, even if vibrational equilibration occurs more rapidly than BET. For example, Fig. 6 implies that β_{DA}° is much less than β_{DA} for the $d\pi$ – $d\pi$, D–A complexes, and this is a plausible result of $\lambda_{DA} < \lambda_{CT}$ [42]. It should also be observed that the simple semi-classical vibronic model used here does not explicitly take vibrational quantization into account, but it seems obvious that in order to be consistent with this model β_{DA} would also be expected to vary with the vibrational state.

Another issue that needs to be investigated is the issue of vibrational structure on the DACT absorption band. An advantage of the CN[−] ligand in this regard is that there are few vibrational modes to consider (one or two), and the intensities are expected to be large. A problem with these systems is that the absorption envelope is the convolution of several electronic components (as many as 12 in some complexes) with relatively small spacings (we would estimate 10–500 cm^{−1}) so that even here the vibronic structure might be very difficult to resolve. Of course, the coupling of ν_{CN} with skeletal, or other, modes would further complicate this situation.

6.2. Extensions to other systems

It seems natural to note the qualitative similarities between our observations on CN-bridged complexes and those of Curtis and co-workers on complexes with aromatic bridging ligands, and to infer that this suggests a significant vibronic component to strong D–A coupling when the bridging ligands are complex aromatic molecules. While there seem to be fewer convenient probes of the bridging ligand involvement in D–A coupling (e.g. shifts in BL vibrational frequencies have not, to our knowledge, been reported), one could cite the larger C–N bond lengths of the bridging pyrazine in $[Ru(NH_3)_5]_2pz^{5+}$ than in either the fully oxidized or fully reduced analog [64] as an indication of very closely related behavior. As noted

above, Piepho [55,56] has used a vibronic model to describe this type of system. This type of system has also been described using three state models [9,65,66] and a wave packet model [67]. These various approaches have focused mostly on the spectroscopy of the Creutz-Taube ion, and even with this limited perspective there is little agreement on the best approach [68–70]. These approaches probably should be viewed as involving somewhat different approximations; the basic question is whether some limited class of approximations are most useful in describing the experimental observations, or whether most, or all, of these seemingly different approaches do each provide insight into different aspects of the behavior of D–A systems. In the same general philosophical spirit, the simple semi-classical model sketched above combines some elements of the vibronic and three state models. This enables us to describe how the bridging ligand can actively promote strong D–A coupling. Some such integrated approach seems necessary to treat a broad range of observations.

Acknowledgements

Partial support by the Division of Chemical Sciences, Office of Basic Energy Sciences, Office of Energy Research, US Department of Energy, of the research performed at Wayne State University is gratefully acknowledged. We have also benefited from discussions of some of our work with Dr. V. Swayambunathan and Professor H.B. Schlegel.

References

- [1] M.A. Fox and M. Channon (eds.) *Photoinduced Electron Transfer*, Elsevier, Amsterdam, 1988, Parts A–D.
- [2] M.D. Newton and N. Sutin, *Ann. Rev. Phys. Chem.*, **35** (1984) 437.
- [3] C. Creutz, *Progr. Inorg. Chem.*, **30** (1983) 1.
- [4] M.J. Weaver, *Chem. Rev.*, **92** (1992) 463.
- [5] M.R. Wasielewski, *Chem. Rev.*, **92** (1992) 435.
- [6] K.D. Jordan and M.N. Padden-Row, *Chem. Rev.*, **92** (1992) 395.
- [7] S.S. Isied, M.Y. Ogawa and J.F. Wishart, *Chem. Rev.*, **92** (1992) 381.
- [8] J.R. Winkler and H.B. Gray, *Chem. Rev.*, **92** (1992) 369.
- [9] C. Creutz, M.D. Newton and N. Sutin, *J. Photochem. Photobiol. A: Chem.*, **82** (1994) 47.
- [10] F.C. DeSchryver, D. Declercq, S. Depaelelaere, E. Hermans, A. Onkelinx, J.W. Verhoeven and J. Gelan, *J. Photochem. Photobiol. A: Chem.*, **82** (1994) 71.
- [11] R.J. Crutchley, *Adv. Inorg. Chem.*, **41** (1994) 273.
- [12] M.D. Ward, *Chem. Soc. Rev.*, (1995) 121.
- [13] R. Billing, D. Rehorek and H. Hennig, *Top. Curr. Chem.*, **158** (1990) 152.
- [14] R. de la Rosa, P.J. Chang, F. Salaymeth and J.C. Curtis, *Inorg. Chem.*, **24** (1985) 4229.
- [15] F. Salaymeth, S. Berhawe, R. Yusof, R. de la Rosa, E.Y. Fung, R. Matamoros, K.W. Law, Q. Zheng, E.M. Kober and J.C. Curtis, *Inorg. Chem.*, **32** (1993) 3895.
- [16] J.F. Endicott, X. Song, M.A. Watzky, T. Buranda and Y. Lei, *Chem. Phys.*, **176** (1993) 427.
- [17] J.F. Endicott, X. Song, M.A. Watzky and T. Buranda, *J. Photochem. Photobiol. A: Chem.*, **82** (1994) 181.

- [18] M.A. Watzky, J.F. Endicott, X. Song, Y. Lei and A. Macatangay, 35 (1997) 3463. *Inorg. Chem.*
- [19] M.A. Watzky, Ph.D. Dissertation, Wayne State University, 1994.
- [20] R.D. Cannon, *Electron Transfer*, Butterworth, London, 1980.
- [21] J.F. Endicott, in R.B. King (ed.), *Encyclopedia of Inorganic Chemistry*, Vol. 3, Wiley, London, 1994, p. 1081.
- [22] R.A. Marcus and N. Sutin, *Biochim. Biophys. Acta*, 811 (1984) 265.
- [23] G.L. Closs and J.R. Miller, *Science*, 240 (1988) 440.
- [24] R.A. Marcus, *Annu. Rev. Phys. Chem.*, 15 (1994) 155.
- [25] N.S. Hush, *Electrochim. Acta*, 13 (1968) 1005.
- [26] R.S. Mulliken and W.B. Person, *Molecular Complexes*, Wiley-Interscience, New York, 1967.
- [27] M.D. Newton, *Chem. Rev.*, 91 (1991) 767.
- [28] T. Buranda, Y. Lei and J.F. Endicott, *J. Am. Chem. Soc.*, 114 (1992) 6916.
- [29] T. Buranda, work in progress.
- [30] K. Tominaga, D.A.V. Kliner, A.E. Johnson, N.E. Levinger and P.F. Barbara, *J. Phys. Chem.*, 98 (1993) 1228.
- [31] P.J. Reid, C. Silva, P.F. Barbara, L. Korki and J.T. Hupp, *J. Phys. Chem.*, 99 (1995) 2609.
- [32] X. Song, Y. Lei, S. Van Wallendael, M.W. Perkovic, D.C. Jackman, J.F. Endicott and D.P. Rillema, *J. Am. Chem. Soc.*, 97 (1995) 3225.
- [33] S.K. Doorn, D.O. Stoutland, R.B. Dyer and W.H. Woodruff, *J. Am. Chem. Soc.*, 114 (1992) 3133.
- [34] S.K. Doorn, R.B. Dyer, D.O. Stoutland and W.H. Woodruff, *J. Am. Chem. Soc.*, 115 (1993) 6398.
- [35] J.P. Fackler, in R.B. King (ed.), *Encyclopedia of Inorganic Chemistry*, Vol. 5, 1994, p. 2270.
- [36] D.E. Richardson and H. Taube, *Coord. Chem. Rev.*, 60 (1984) 107.
- [37] A. Haim, *Comments Inorg. Chem.*, 4 (1984) 113.
- [38] D.E. Richardson and P. Sharpe, *Inorg. Chem.*, 32 (1993) 1809.
- [39] D.E. Richardson, *Inorg. Chem.*, 29 (1990) 3213.
- [40] G. Naray-Szabo and G.G. Ferenczy, *Chem. Rev.*, 95 (1995) 829.
- [41] J. Shaw and G.W. Everett, *Inorg. Chem.*, 24 (1985) 1917.
- [42] M.A. Watzky and J.F. Endicott, in preparation.
- [43] C.A. Bignozzi, R. Argazzi, J.R. Schoonover, R.B. Dyer and F. Scandola, *Inorg. Chem.*, 31 (1992) 5260.
- [44] M.A. Watzky and J.F. Endicott, *Inorg. Chim. Acta*, 226 (1994) 109.
- [45] C.A. Bignozzi, S. Roffia and F. Scandola, *J. Am. Chem. Soc.*, 107 (1985) 1644.
- [46] S. Roffia, C. Paradisi and C.A. Bignozzi, *Electroanal. Chem. Interfacial Electrochem.*, 200 (1986) 105.
- [47] W.L. Parker and G.A. Crosby, *Int. J. Quantum Chem.*, XXIX (1991) 299.
- [48] U. Furholz, H.-B. Burgum, F.E. Wagner, A. Stebler, J.H. Ammeter, E. Krausz, R.J.H. Clark, M.J. Stead and A. Ludi, *J. Am. Chem. Soc.*, 106 (1984) 121.
- [49] K. Nakamoto, *Infrared and Raman Spectra of Inorganic and Coordination Compounds*, Wiley, New York, 4th edn., 1986.
- [50] I.B. Bersuker, *The Jahn Teller Effect and Vibronic Interactions in Modern Chemistry*, Plenum, New York, 1989.
- [51] G. Fischer, *Vibronic Coupling*, Academic Press, New York, 1984.
- [52] C.J. Ballhausen, in C.D. Flint (ed.), *Vibronic Processes in Inorganic Chemistry*, Kluwer, Dordrecht, 1989, p. 53.
- [53] M. Bixon, J. Jortner and J.W. Verhoeven, *J. Am. Chem. Soc.*, 116 (1994) 7349.
- [54] R.G. Vekhter and M.A. Ratner, *J. Phys. Chem.*, 99 (1995) 2656.
- [55] S.B. Piepho, *J. Am. Chem. Soc.*, 110 (1988) 6319.
- [56] S.B. Piepho, *J. Am. Chem. Soc.*, 112 (1990) 4197.
- [57] R.I. Cukier, *J. Phys. Chem.*, 99 (1995) 945.
- [58] R.I. Cukier, *J. Phys. Chem.*, 98 (1994) 2377.
- [59] A.P.B. Lever, *Inorganic Electronic Spectroscopy*, Elsevier, New York, 2nd edn., 1984.
- [60] J.J. Alexander and H.B. Gray, *J. Am. Chem. Soc.*, 90 (1968) 4260.
- [61] H.B. Gray and N.A. Beach, *J. Am. Chem. Soc.*, 85 (1963) 2922.
- [62] D.F. Gutterman and H.B. Gray, *Inorg. Chem.*, 11 (1972) 1727.
- [63] J.J. Alexander and H.B. Gray, *Coord. Chem. Rev.*, 2 (1967) 29.

- [64] U. Fürholz, J. Joss, H.B. Bürgi and A. Ludi, *Inorg. Chem.*, 24 (1985) 943.
- [65] L.T. Zhang, J. Ko and M.J. Ondrechen, *J. Am. Chem. Soc.*, 109 (1987) 1666.
- [66] M.J. Ondrechen, J. Ko and L.T. Zhang, *J. Am. Chem. Soc.*, 109 (1987) 1672.
- [67] C. Simani, C. Reber, D. Talaga and J.I. Zink, *J. Phys. Chem.*, 97 (1993) 12678.
- [68] P.N. Schultz and S.B. Piepho, *J. Phys. Chem.*, 98 (1994) 11226.
- [69] M.J. Ondrechen, A. Ferretti, A. Lami and G. Villani, *J. Phys. Chem.*, 98 (1994) 11230.
- [70] D.S. Talaga, C. Reber and J.I. Zink, *J. Phys. Chem.*, 98 (1994) 11233.